

Sampling the energy landscape of Pt₁₃ with metadynamics^{*}

Luca Pavan, Cono Di Paola, and Francesca Baletto^a

Department of Physics, King's College London, London, WC2R 2LS, UK

Received 7 September 2012 / Received in final form 27 November 2012

Published online (Inserted Later) – © EDP Sciences, Società Italiana di Fisica, Springer-Verlag 2013

Abstract. The potential energy surface of a metallic nanoparticle formed by 13 atoms of platinum is efficiently explored using metadynamics in combination with empirical potential molecular dynamics. The scenario obtained is wider and more complex of what was previously reported: more than thirty independent energy basins are found, corresponding to different local minima of Pt₁₃. It is demonstrated that in almost all the cases these motifs are local minima even at ab-initio level, hence proving the effectiveness of the method to sample the energy landscape. A classification of the minima in structural families is proposed, and a discussion regarding the shape and the connections between energy basins is reported.

1 Introduction

Metallic nanoparticles (NPs) constitute an important and relatively new multidisciplinary research field, encompassing physics, chemistry and engineering. This field is constantly expanding thanks to potential technological applications, such as nano-catalysis, DNA-sequence sensors, antimicrobial applications and nano-devices for magnetic storage [1–4]. It is noted that the physical and chemical properties of NPs, which differ both from those of single molecules and the bulk metals [5], are size, shape and composition dependent, thus creating the fascinating possibility of tailoring novel materials to satisfy a particular technological need. Since the geometry that best effects the requirement could be one among the enormous variety of possible structural combinations that the system can assume, a knowledge of the conformational space of metal NPs is fundamental to control physical and chemical properties, and the subsequent development of new technological applications [6,7].

The search for the most favourable or best structure at 0 K, corresponding to the global minimum of the potential energy surface (PES), for a given size and chemical composition, is a non-polynomial hard problem, since the number of different isomers depends on $N!$, where N is the number of atoms in the cluster itself. Many techniques have been developed to sample the PES, such as genetic algorithm and basin hopping [8,9]. These techniques, combined with density-functional-theory calculations, have been successfully used to find the putative global minima for small Pt clusters [10]. However, the exploration of the free energy surface (FES) of a metallic

NP is still in its infancy [6,11]. A possibility resides in the use of metadynamics, an algorithm used to bias the dynamics of a system through a history dependent potential, in order to accelerate rare events in a molecular dynamics simulation, sample the configurational space and efficiently explore the FES. Since its introduction [12], the method has been applied in biophysics, chemistry, crystal structure prediction and material science [13]. Although very powerful, metadynamics has been used infrequently in the case of metallic NPs [6,14].

This work concentrates on the implementation of the metadynamics algorithm to sample the energy landscape of Pt₁₃, using the coordination number as unique collective variable and describing the interatomic interaction through an empirical potential. The energy ordering is then calculated at ab-initio level in a spin-polarised framework. While previous studies are devoted to the search of the putative global minimum over a wide size range [15–19] or regarding the transition between planar and spherical shapes [20], a full picture of the landscape of Pt₁₃ is reported here. This is followed by a classification in structural families based on a geometrical analysis of the local environment of each pair of nearest neighbour. In addition, an analysis of energy basin shapes and their connections is presented.

2 Method

Metadynamics (MT) is an algorithm consisting in a molecular dynamics (MD) simulation coupled with a history dependent potential. It can be used to accelerate rare events, that are occurrences characterised by a much longer time scale than the one of the time step of the simulation. Moreover, it can be exploited to reconstruct the FES of the system. The algorithm is based on a dimensional reduction, and works in the following way [13]: given a system, described by a set of coordinates \mathbf{r} and a potential $V(\mathbf{r})$, that

^{*} ISSPIC 16 - 16th International Symposium on Small Particles and Inorganic Clusters, edited by Kristiaan Temst, Margriet J. Van Bael, Ewald Janssens, H.-G. Boyen and Françoise Remacle.

^a e-mail: francesca.baletto@kcl.ac.uk

evolves subjected to a dynamics, a proper set of collective variables (CVs) has to be chosen, in a way that they are continuous and derivable functions of \mathbf{r} . Every time step τ_G , a small repulsive Gaussian potential is added to the potential $V(\mathbf{r})$, centred along the trajectory followed by the chosen set of CVs, so at time t the metadynamics potential acting on the system is the sum of all the Gaussians deposited.

In this study, only one CV is used to sample the PES of Pt₁₃ and to detect the shape of its energy basins, the total coordination number (CN), which is the sum of the number of nearest neighbours of every atom forming the cluster. It is a geometry related variable, very useful and employed to explore and distinguish chemical reaction pathways [13]. The following analytic expression of CN is employed:

$$CN = \sum_{i,j} \sum_{i \neq j} f(r_{ij}) \quad (1)$$

$$f(r_{ij}) = \begin{cases} 1 & \text{if } r_{ij} \leq d_0, \\ 1 - \left(\frac{r_{ij} - d_0}{r_0} \right)^n & \text{if } r_{ij} > d_0, \\ \frac{1 - \left(\frac{r_{ij} - d_0}{r_0} \right)^n}{1 - \left(\frac{r_{ij} - d_0}{r_0} \right)^m} & \text{if } r_{ij} > d_0, \end{cases} \quad (2)$$

where d_0 is the nearest neighbour bulk reference distance, r_0 is a distance related to the width of the descending branch of the function, n and m are parameters used for tuning its smoothness and asymptotic behaviour. In this work, $d_0 = 1/\sqrt{2}$ and $r_0 = 0.147$, where both values are referred to Pt face centred cubic bulk lattice parameter $a_{FCC}^{Pt} = 3.917$ Å, $m = 12$ and $n = 6$.

The choice of this coordinate reduction, based on one CV, does not satisfy all the constraints needed to correctly reconstruct the FES [13], but it reveals itself to be enough to permit an efficient exploration of the PES, if many simulations are performed from different starting configurations.

The Pt-Pt interactions are modelled using the Rosato-Guillopé-Legrand empirical many-body potential (EP), derived within the second moment approximation to the tight-binding model [21], where the total potential energy, E_{tot} , is expressed as a sum, over all the atomic pairs, of two terms,

$$E_{tot} = \sum_i \sum_j A e^{-p \left(\frac{r_{ij}}{r_0} - 1 \right)} - \sqrt{\xi^2 e^{-2q \left(\frac{r_{ij}}{d_0} - 1 \right)}}, \quad (3)$$

where r_{ij} is the distance between the atomic sites i and j and d_0 is the nearest neighbour reference distance in the bulk. The potential parameters, A , ξ , p , q , are fitted to several bulk experimental values, such as the cohesive energy ϵ_{coh} , the lattice parameter, and the elastic constants, as the bulk modulus, C44, and C. For platinum atoms the following values are used: $A = 0.2744$ eV, $p = 10.71$, $\xi = 2.6210$ eV, $q = 3.845$ and $d_0 = 2.77$ Å [22].

The simultaneous satisfaction of the two opposite requirements of computational speed and accuracy in

the sampling of the PES is reached using the values $h_G = 5$ meV and $\delta_G = 0.1$ (CV unit) as, respectively, height and width of the metadynamics potential Gaussians, and time interval $\tau_G = [10-15]$ ps. Being interested in the potential energy landscape, only temperatures as low as 5 ± 2 are considered. Additionally, to ensure a detailed investigation, an iterative procedure is performed, where different initial configurations are chosen. This is done in the following way: empirical potential metadynamics (EP-MT) simulations are performed starting from different initial configurations, previously ionic relaxed; during the first set of simulations the system explores many energy basins, some of them belonging to new geometrical structures, each of which is subsequently relaxed to its closest minimum. In addition, short (50 ps) EP-MD simulations at constant temperature are performed for all of them, in order to test their thermal stability at different temperatures, and to get, sometime, further geometries to be used as new initial configurations. A second set of EP-MT simulations are performed using the so obtained isomers as new initial configurations, in an iterative way.

The initial starting configurations are: icosahedron (Ih), ino-decahedron (Dh) [23], cuboctahedron (Co), the buckled pyramid, labelled as M4 in Figure 1, that is suggested to be the lowest energy structure at density functional (DF) level [18] and an assembly of simple cubes [19], resulting to be a distorted poly 6 atom octahedron penetrated by a 7 atom decahedron after quenching, hereinafter named M11, that is a deformation of the isomer labelled as M16.

Independent EP-MT simulations are collected varying the initial velocities of the atoms, in order to see if there are differences in the order of exploration of the energy basins. It turns out that this leads to a partially different series of visited minima, increasing the sampling capability of the method itself. However, since the iterative approach has been found to be faster, this has been preferentially performed.

All the isomers are characterised through the calculation of the total coordination number, the distances of the nearest and furthest atoms from the centre of mass, and by common neighbour analysis (CNA) [24], which examines the local surroundings of each pair of nearest neighbours (NNs) forming the NP. It works giving a signature to each pair of NNs, consisting of a triplet of integers r , s , t , where r is the number of NNs common to both of the atoms of the pair, s is the number of NN pairs found among the r atoms, and t is the length of the longest chain that can be built bonding together the s atoms if they are NNs. The morphology of a cluster is identified by the comparison of percentages of pairs sharing selected signatures with values belonging to referential models.

3 Results and discussion

The potential energy landscape of Pt₁₃ plotted versus the total coordination number is reported in Figure 1. Each local minimum is indicated by a mark, whose shape refers to the family it belongs to, and labelled with M followed

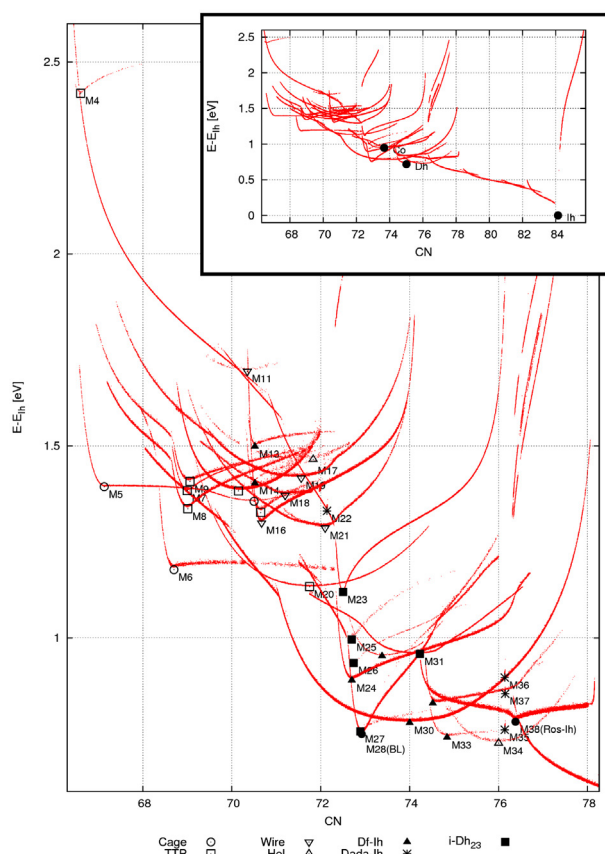


Fig. 1. PES of Pt_{13} as a function of the coordination number. The main plot shows the isomers characterised by a low coordination number, while the whole figure is reported in the inset. Local minima are marked using different symbols to identified the families they belong to: Cage (circle), TTP (square), Wire (downward pointing triangle), helicoid-like (upward pointing triangle), Df-Ih (black triangle), Dada-Ih (asterisk), i-Dh₂₃ (black square). A black circle is used for all the single component families, like BL, Ros-Ih and Ih. All the hollow symbols marks the isomers of the hollow and open structures group. If a structure is simply a deformation of some other motif, only the latter is labelled.

by an integer, except for Ih, Dh and Co. If a structure is simply a deformation of some other motif, only the latter is labelled. It is worth noting that Co and Dh are not truly stable and rapidly evolve into an Ih, therefore, all the simulations having them as initial configuration can be considered as starting from an Ih basin.

The iterative metadynamics simulations proposed here, although restricted to one CV, and using a classical empirical potential, give access to a wide range of motifs. In Figure 2, where isomers are sorted according to the descending order of their energy values, it can be seen that the conformational space is explored towards energies that are both higher and lower than the one of the starting configuration; nonetheless the process is more efficient going towards less energetic structures. This is consistent with the way the metadynamics algorithm works [13]: to go higher in energy more Gaussians are needed and more time have to be waited.

	M4	M11	M14	M22	M21	M23	M36	M37	M30	M27	M34	Ih
M4	●											
M11		●										
M13					△							
M17					△							
M19			△									
M9				△	△							
M14		●										
M5					△	△						
M7						△	△				△	
M18				△								
M8				△								
M22				●								
M16			▽									
M21					●							
M6	▽	▽				△			△			△
M20						△						
M23	▽					●						
M25	▽											
M31						▽						
M26	▽											
M36							●					
M24	▽	▽	▽	▽	▽	▽		△	△	△	△	△
M37								●				
M38	▽	▽				▽	▽		△			△
M30	▽	▽						▽	●	△		△
M35		▽			▽							
M27								▽		●		
M28						▽					△	
M33	▽	▽	▽	▽	▽	▽	▽	▽	▽	▽	△	△
M34	▽	▽	▽	▽	▽	▽	▽	▽	▽	▽	●	△
Ih	▽	▽	▽	▽	▽	▽	▽	▽	▽	▽	▽	●

Fig. 2. Results of the simulations performed to explore the PES of Pt_{13} . The starting points of the simulations are indicated in the column headers, sorted according to the descending order of their energy values. If an isomer is found starting from one of them, a mark is drawn in the corresponding row. A \triangle indicates a minimum that is more energetic than the starting configuration, a ∇ marks a less energetic one, and a circle shows the initial configuration.

The adopted empirical potential is known to favour highly coordinated geometries being fitted on bulk parameters [22,25]. On the other hand, small Pt clusters prefer low coordinated ones, once studied at DF level. Nonetheless, the iterative EP-MT is shown to be able to find many and various hollow and open shapes, which result to be local minima of the potential itself. MT is not constrained to move towards the most energetically favourable ones, as other algorithms, dedicated to the global minimum search, do. This is an important quality of the method, because the semi-empirical potential used is computationally really fast, although it is not always able to reproduce the correct energy order of the minima. Using EP-MT simulations to find a wide range of structures that are subsequently relaxed at density functional level, is an accurate and economic solution to get a detailed sampling of energy landscape of metallic nanoparticles.

3.1 Classification of the Pt_{13} isomers

All minima that are not resulting from a simple deformation of some other motif, called using their labels, are classified into families following geometrical considerations, such as the evaluation of the quantity Δ , defined

Table 1. Differences between the maximum and minimum distance from the centre of mass Δ [Å] and CNA signatures, in %, for the Pt₁₃ families, divided by group. Bulk signatures *555*, *433*, *422* characterise non-crystallographic environment, while *421* is typical of FCC geometries. Surface signatures *322*, *311* and *300* are associated with (111) facets, *211* with (100), and *200* with (110).

Family	Δ [Å]	<i>555</i>	<i>433</i>	<i>422</i>	<i>421</i>	<i>322</i>	<i>311</i>	<i>300</i>	<i>211</i>	<i>200</i>
Ih	2.4	28.6	0.0	0.0	0.0	71.4	0.0	0.0	0.0	0.0
Ros-Ih	2.4	10.5	10.5	0.0	0.0	44.7	5.3	0.0	21.1	0.0
Df-Ih	2.1–3.4	0.0–8.1	5.4–11.1	0.0–5.7	0.0	18.9–40.5	5.4–27.0	0.0	10.8–22.9	17.1–18.9
Dada	1.7–2.8	8.3–13.2	18.4–22.2	0.0	0.0	38.9–47.4	0.0	0.0	21.1–30.6	0.0
Co	2.5	0.0	0.0	0.0	33.3	0.0	0.0	0.0	66.7	0.0
BL	2.1	0.0	0.0	0.0	8.3	0.0	41.7	0.0	8.3	41.7
Dh	2.6	5.4	0.0	27.0	0.0	27.0	0.0	0.0	27.0	0.0
i-Dh ₂₃	2.0–8	0.0–2.8	0.0–10.8	5.4–11.1	0.0	11.1–25.0	16.7–41.7	0.0–2.8	13.9–25.0	8.3–33.3
Cage	1.5–1.6	0.0	0.0	0.0	0.0	0.0–8.8	0.0–11.8	0.0	0.0–5.9	73.5–100.0
TTP	1.6–2.8	0.0	0.0	0.0	0.0	0.0	14.7–36.4	0.0–5.9	2.9–36.4	27.3–76.5
Wire	2.3–2.7	0.0–2.8	0.0–16.7	0.0–2.8	0.0–2.9	17.1–30.6	13.9–34.3	0.0	17.1–25.0	8.3–25.7
Hel	2.4–2.8	2.8–7.9	10.5–13.9	2.6–2.8	0.0–2.8	30.6–39.5	10.5–13.9	0.0	13.2–25.0	8.3–13.2

as the difference between the maximum and minimum distance from the centre of mass, and the CNA signatures. These quantities are reported in Table 1.

The families can be further organised into four main groups: icosahedra (Fig. 3), decahedra, crystallographic motifs (both these two groups are shown in Fig. 4), and hollow and open shapes (Fig. 5). The proposed classification is reported below:

- group of icosahedra, formed by the following families:
 - icosahedron (Ih),
 - rosette motif (Ros-Ih) M38, where a 5-fold vertex is lost in order to form a hexagonal ring [25],
 - simple defected Ih (Df-Ih): if 1 or 2 defects are present on the surface of an Ih, at least one of which, if they are bound, has less than 4 nearest neighbours,
 - Dada-Ih: at least 2 bound defects are present on the surface of an Ih, none of which having less than 4 nearest neighbours;
- group of decahedra, made up by:
 - ino-decahedron (Dh),
 - incomplete 23 atom decahedra (i-Dh₂₃);
- group of crystallographic face centred cubic (FCC) motifs, constituted by:
 - cuboctahedron (Co),
 - bi-layer face centred cubic structure (BL), labelled M28;
- group of hollow and open shapes, formed by the following families:
 - cage-like (Cage): characterised by a small difference between the maximum and minimum distance from the centre of mass,
 - triaugmented triangular prism based (TTP): structures sharing a core formed by pyramids attached to the square facets of a triangular prism,
 - wire-like (Wire), which are isomers with high aspect ratio, some of them having an icosahedral core, as M18, some formed by a chain of 7 atom

decahedra, as M21, or being made by 6 atom octahedra, as M16,
– helicoid-like (Hel).

The family of simple defected Ih is formed by M24, M30, M33, M13 and M14. M30 has a 2-fold symmetry axis, M24 and M14 a reflection plane. They are characterised by no FCC bulk signature combined with generally medium values of *555*, and *433* lower than 12%. The Dada-icosahedra are labelled M35, M22, M37 and M36. They are part of an Ih penetrated with a seven atom decahedron, but they could be also seen as part of a Pt₁₉ double-icosahedron. This family is named after the similarity of M35 with “Bicycle Wheel”, by the Dadaist artist Duchamp [26]. This class is marked by the highest *555*, after Ih and Ros-Ih, and *433* (above 18%). Other bulk signatures are absent. The surface shows no *311*, *300* and *200*, but high values of *322* and *211*. The bottom of the energy basins of this class of isomers is particularly spiky, resembling the one of Ih, as depicted in Figure 1. Searching a relationship between this feature and the results of CNA, it can be found that the sum of bulk signatures *555* and *433* is greater than 28% for all, and only for, these isomers and Ih. M38, the Ros-Ih, has one reflection symmetry plane and it is marked by the second highest value of *555* bulk signature after the Ih. Its *322* surface signature is really high, on the same level with the Dada-icosahedra.

The i-Dh₂₃ family, that with the Dh forms the decahedral group, consists of M23, M25, M26, M27, and M31. A part from the latter, that could be also considered a Df-Ih, they have the highest range of values of bulk signature *422*, typical of the Dh. M23 is a truncated bi-pyramid, an highly symmetric structure, having 3 reflection planes of symmetry and a 3-fold axis; M27 has 2 perpendicular reflection planes, M25 and M26 only one.

The group of face centred cubic motifs is formed only by two structures: the Co and the BL, M28. It is a highly symmetric structure as the truncated bi-pyramid M23, having 3 reflection planes and a 3-fold rotational axis. Its only bulk signature is the *421*, being crystallographic;

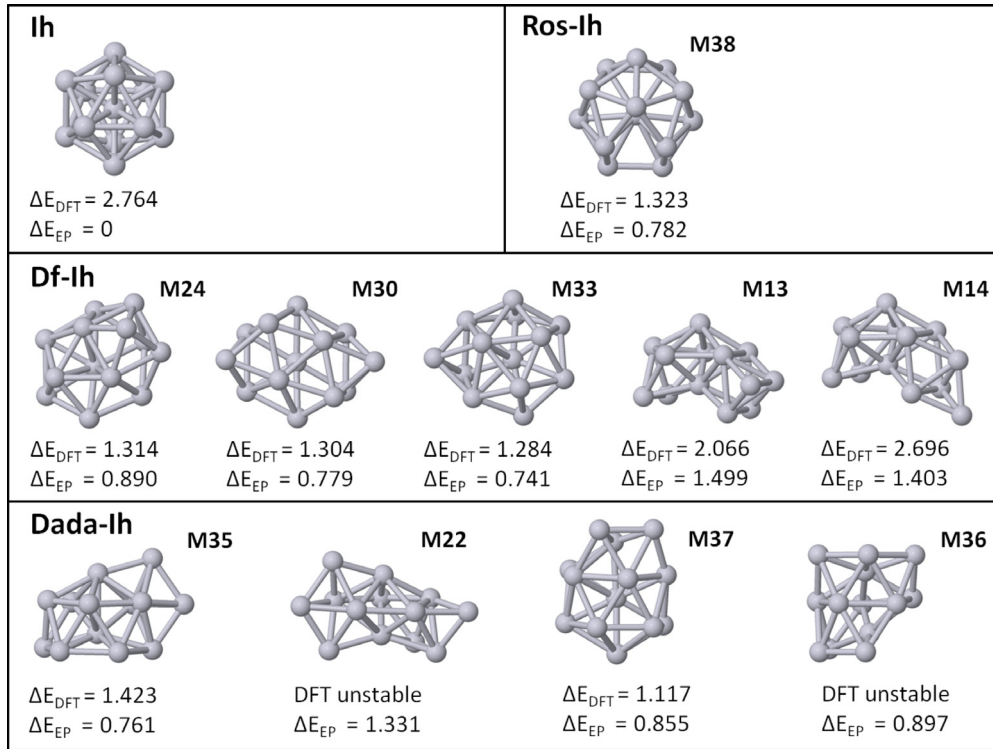


Fig. 3. Families of the icosahedral group. The energetic stability of each motifs is reported in eV, both at empirical (EP) and density-functional (DFT) level, with respect to the putative global minimum, that is Ih in the first case, and M4 (TTP) in the second.

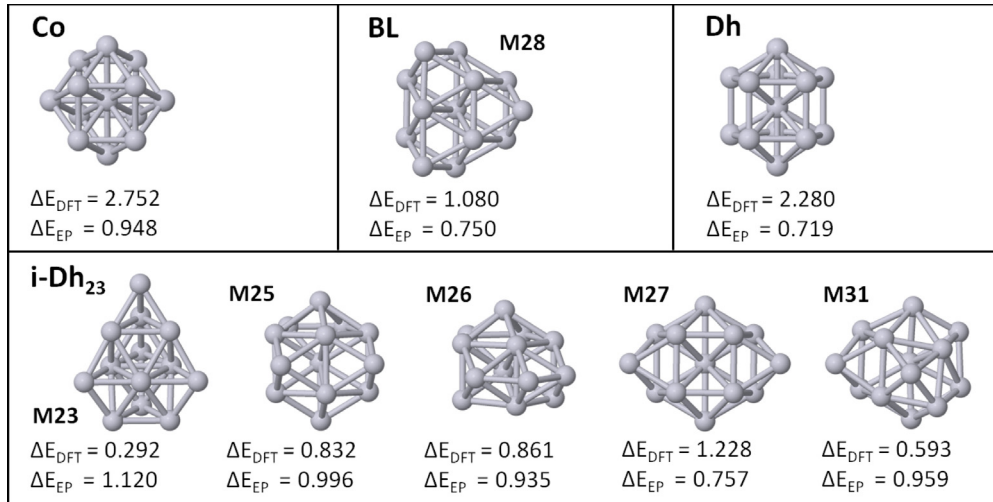


Fig. 4. Families of the crystallographic (Co and BL) and decahedral groups (Dh and i-Dh₂₃). Energy values follow the same convention as in Figure 3.

311 surface signature has the highest value, 41.7%, as in the case of M23. The cage-like family, in the hollow and open shape group, is formed by isomers M5 and M6, having two perpendicular reflection planes of symmetry. It has the highest values of the 200 signature, the one characterising (110) planes: above 73%; furthermore, among all the structures, M6 is the one with the smallest difference between maximum and minimum distances from the centre of mass, as shown in Table 1. This feature, with the fact that these arrangements do not have any

nearest neighbour pairs of atoms with a bulk signature, makes them cage-like. In the same group, the TTP family consists of isomers M4, M7, M8, M9 and M20. M4 has a 2-fold rotational axis and two perpendicular symmetry planes, M7 and M8 have only one. These two isomers, together with M9 and M20, are formed by a six atom octahedron attached to the characteristic triaugmented triangular prism. This particular geometry causes this subset of structures to have the highest values of 300 surface signature: 5.9%. This feature is really

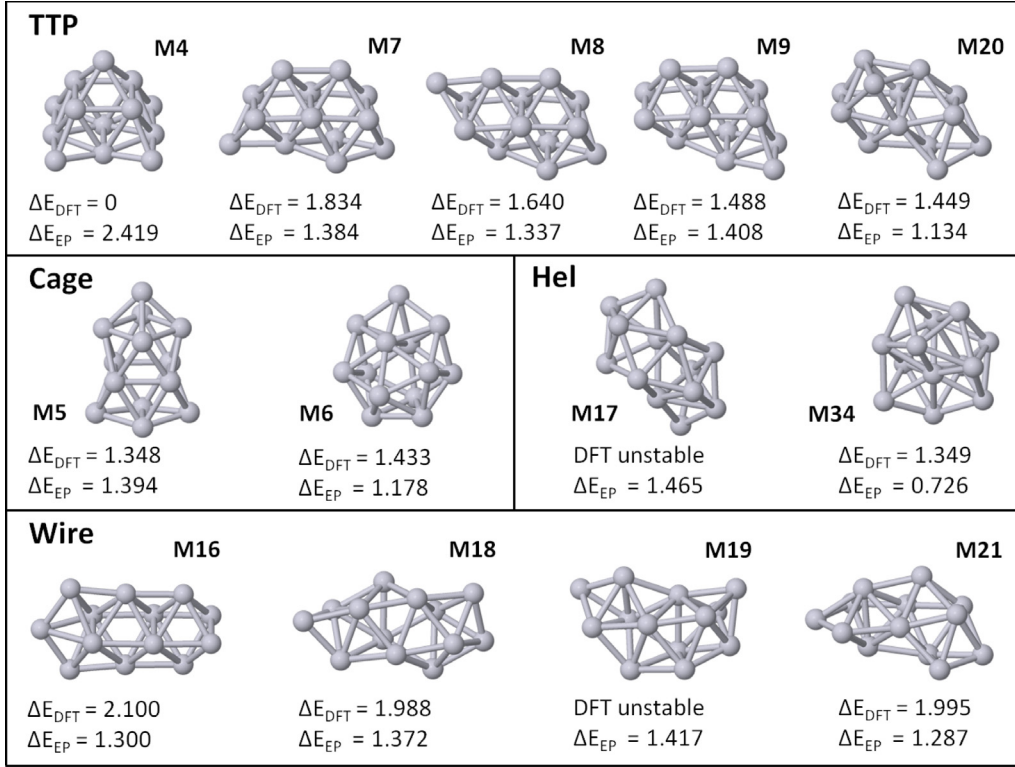


Fig. 5. Families of the hollow and open shape group. Energy values follow the same convention as in Figure 3.

peculiar because 300 signature is absent from almost all the arrangements, except stellations or deformations of decahedra. This family has not got pairs of neighbours with bulk signatures, and high 200 signature, ranging from 27% to 77%, like the cage-like family. Unlike that class, it has no 322 , and rather high values of 311 . The wire-like family is formed by the open structures M16, M18, M19, M21. M16 is a poly 6 atom octahedron penetrated by a 7 atom decahedron, the most symmetric structure among this group, having two perpendicular reflection planes. Unlike the other members of its class, it does not show any bulk signature a part from a rather high 2.9% of 421 , associated with the FCC arrangement. All the other isomers are marked by high percentage of 433 non crystallographic bulk signature; low 421 is generally present, while it is completely absent from all non crystallographic structures belonging to the other groups. In the cases of M21 and M19 low 555 can be found. The helicoid-like family complete the group, and consists of M17 and M34. Their atoms are arranged along two helicoids around one central axis, but defects are present; M34 could be seen also as an incomplete and distorted hexagonal antiprism. Their signatures are similar to the ones of wire-like structures.

3.2 Energy ordering

All the Pt_{13} isomers obtained, are ionically relaxed at density functional level, using the plane wave code in the QUANTUM ESPRESSO distribution [27]. The Broyden-Fletcher-Goldfarb-Shanno (BFGS) procedure is

applied. The generalised gradient approximation (GGA) with the Perdew-Burke-Ernzerhof (PBE) functional [28] is employed with an energy cutoff of 45 Ryd and a charge density cutoff of 360 Ryd. Ultrasoft pseudo-potential are included for Pt atoms with an electronic configuration $5d^9 6s^1$, and all the calculations are performed at Γ point. Spin polarised calculations have been found to estimate correctly the total magnetisation with respect to relativistic approaches, including the spin-orbit coupling [29].

In Figures 3, 4 and 5, the differences of energies with respect to the putative global minimum, both at semi-empirical and ab-initio level, are shown. The global minimum is the Ih in the first case, and M4, of the TTP family, in the second. The energy ordering is expected to be different, due to the delocalisation of the d-electrons, which favours hollow structures, considered only at DF level. However, except in the few cases of the Dada-Ih M22 and M36, the helicoid-like M17 and the wire-like M19, the geometries found using the MT procedure have been preserved even after the ionic relaxation at DF level, suggesting that the method is an efficient way to explore the PES of metallic nanoparticles.

3.3 Shape and connection of energy basins

As Figure 1 shows, the bottom of the energy basins can be shaped in three different ways, classified in the following way:

- “V” shaped, like the basin of M23,

- spiky shaped, like the Ih, when it is particularly steep,
- “U” shaped, like M30, when the bottom of the basin is almost flat,
- “L” shaped, like the M5, when it is flat in one direction, and steep in the opposite one.

A connection between spiky shaped energy basins and signatures has been conjectured when speaking about Dada-Ih: the signatures 555 and 433, related to an atomic neighbourhood rich and bound seems to match “stiff” Pt₁₃ isomers. Being this relationship based on a purely geometrical property, it should be potential independent. However, it has to be checked how much the basin shape modification is emphasised by the parameters of the semi-empirical potential. Moreover, the fact that there could be a relationship between signatures and basin shapes could be supported by the fact that an high value (greater than 34%) of 311 surface signature seems to be related to V shaped basins; the case of M27 (i-Dh₂₃) and M28 (BL) is exemplary: they have almost the same energy and CN, and their basins are shaped in a very different way. The isomer that has a higher value of 311, M28, is associated with a “V”, peaked energy basin, the other with a flatter one. However, the difference in the shapes of the basins could be due to the fact that M28 has also a larger number of symmetries than M27. The cage-like M5 and M6, the structure belonging to the TTP family M4 and the wire-like M16 have the same symmetries and are low coordinated; also in this case, the isomers with higher values of 311 signature match with spikier basins.

The results of the simulations performed to explore the PES, as presented in Figure 2, show that most of the basins seems to be connected at least in one direction: only isomers M4, M11, M14, M21, M22, M36, M37 are not found starting from a different structure, however starting from them many others are met. M4 and M11 are motifs highly energetic, chosen from previous studies as starting configurations, the others are obtained through MD simulations performed to escape from the basins of other structures, as described in Section 2. The energy barriers to enter in the basins of this set of isomers is high, when an EP-MT simulation accelerates the motion of the system only along the collective variable CN.

Among all the other isomers found with MT, some of them are found starting from different point; they are: Ih, M5, M6, M7, M9, M24, M28, M30, M33, M34, M35, M38. In particular Ih, M6, M24, M30, M33, M34, M38 are the most frequent. In general they are among the most stable shapes at each coordination number. In addition, with the exception of Ih, they are characterised by similar binding energies, both at DF and EP levels, suggesting that their coexistence is likely to happen at finite temperatures.

The MD simulations at different temperatures performed on the isomers show that all the members of the cage-like family and M11 (Wire) have very low stability, in fact they easily escape their basins if kept at temperatures below 50 K for 50 ps. Other isomers that exhibit the same behaviour, but in a range of temperatures between 50 and 100 K are M17 (Hel), and the Df-Ih M33.

This results are consistent with the shapes of their energy basins calculated through MT simulations (Fig. 1).

Some connections between energy basins can be found both increasing the temperature and accelerating the exploration using MT; some other connection are visible only using one of the two methods. Belonging to the first case are the transformations from the cage-like M5 to a similar isomer, from M6 (cage-like) to the rosette-like M38, from a TTP similar to M9 to M9 itself, M13 (Df-Ih) to M34 (Hel), M19 (Wire) to Ih, from a Df-Ih similar to M24 to M24, from M31 (i-Dh₂₃) to M38 (Ros-Ih), between M33 (Df-Ih) and M34 (Hel) in both directions, and from M37 (Dada-Ih) to M33 (Df-Ih). On the other hand, M8 (TTP) transforms in M30 (Df-Ih) under the effect of temperature, but there is no evidence they are connected along the direction of the collective variable; this in general is true for all the isomers of TTP class and M30. Similar are the cases of M11 (Wire) that evolves in M22 (Dada-Ih), M20 (TTP) transforming in M27 (i-Dh₂₃), M35 (Dada-Ih) in the isomers of the same family M36 and M37, and M36 in M31 (i-Dh₂₃). The cage-like similar to M5 thermally escapes into both the connected basins, as shown by the performed EP-MT simulations, of the two similar isomers M30 (Df-Ih) and M27 (i-Dh₂₃), but EP-MT does not show any connection.

4 Conclusion

The sampling of the potential energy surface of a small metallic nanoparticles is carried out using an iterative metadynamics based on an empirical potential. This method results to be efficient even when only one collective variable, such as the coordination number, is employed. The different isomers so obtained are then energetically ordered throughout density functional ionic relaxation. The iterative EP-MT, tested on the paradigmatic case of Pt₁₃, is shown to be an efficient method, which allows to get useful knowledge about the stability of minima and on the shape and connection of energy basins. A complete classification of the variety of isomers that are found is proposed following geometrical considerations arising by the common neighbour analysis.

An interesting possibility seems to emerge, about the relationship between geometrical structure and the shape of energy basins. This aspect needs a deeper investigation, also considering that basin shapes could be related with phonon modes in clusters. Finally, the probability of coexistence at finite temperatures of particular sets of isomers can be extrapolated from how frequently a structural motif appears and whether it can be obtained from different structural pathways.

This work is supported by the U.K. research council EPSRC, under Grant No. EP/G003146/1. F.B. thank the MP0903 Nanoalloy-COST Action for the financial support to attend the ISSPIC XVI conference in Leuven. The authors would like to thank Dr. A. Comisso for his technical support.

References

1. J.P. Wilcoxon, B.L. Abrams, *Chem. Soc. Rev.* **35**, 1162 (2006)
2. A. Barnard, *Rep. Prog. Phys.* **73**, 086502 (2010)
3. F. Baletto, R. Ferrando, *Rev. Mod. Phys.* **77**, 371 (2005)
4. D.L. Feldheim, C.A. Foss Jr., *Metal Nanoparticles: Synthesis, Characterization, and Applications* (CRC Press, London, 2002)
5. C. Burda, X. Chen, R. Narayanan, M.A. El-Sayed, *Chem. Rev.* **105**, 1025 (2005)
6. G. Santarossa, A. Vargas, M. Iannuzzi, A. Baiker, *Phys. Rev. B* **81**, 174205 (2010)
7. D.J. Wales, *Phil. Trans. R. Soc. A* **370**, 2877 (2012)
8. R.L. Johnston, *Dalton Trans.* **1**, 4193 (2003)
9. D.J. Wales, *Energy Landscapes* (Cambridge University Press, Cambridge, 2003)
10. X. Wang, D. Tian, *Comput. Mater. Sci.* **46**, 239 (2009)
11. F. Calvo, *Phys. Rev. E* **82**, 046703 (2010)
12. A. Laio, M. Parrinello, *Proc. Natl. Acad. Sci. USA* **99**, 12562 (2002)
13. A. Laio, F.L. Gervasio, *Rep. Prog. Phys.* **71**, 126601 (2008)
14. G.A. Tribello, J. Cuny, H. Eshet, M. Parrinello, *J. Chem. Phys.* **135**, 114109 (2011)
15. A. Nie, J. Wu, C. Zhou, S. Yao, R.C. Robert, H. Cheng, *Int. J. Quant. Chem.* **107**, 219 (2007)
16. A. Sebetci, Z.B. Guvenc, *Mod. Sim. Mat. Sci. Eng.* **13**, 683 (2005)
17. E. Aprà, A. Fortunelli, *J. Phys. Chem. A* **107**, 107 (2003)
18. C.H. Hu, C. Chizallet, H. Toulhoat, P. Raybaud, *Phys. Rev. B* **79**, 195416 (2009)
19. L.-L. Wang, D.D. Johnson, *Phys. Rev. B* **75**, 235405 (2007)
20. V. Kumar, Y. Kawazoe, *Phys. Rev. B* **77**, 205418 (2008)
21. V. Rosato, M. Guillopé, B. Legrand, *Philos. Mag. A* **59**, 321 (1989)
22. F. Baletto, R. Ferrando, A. Fortunelli, F. Montalenti, C. Mottet, *J. Chem. Phys.* **116**, 3856 (2002)
23. S. Ino, *J. Phys. Soc. Jpn* **27**, 941 (1969)
24. D. Faken, H. Jonsson, *Comput. Mater. Sci.* **2**, 279 (1994)
25. E. Aprà, F. Baletto, R. Ferrando, A. Fortunelli, *Phys. Rev. Lett.* **93**, 65502 (2004)
26. M. Duchamp, *Bicycle Wheel*, www.moma.org/collection
27. P. Giannozzi et al., *J. Phys. Condens. Matter* **21**, 395502 (2009)
28. J. Perdew, K. Burke, M. Ernzerhof, *Phys. Rev. Lett.* **77**, 3865 (1996)
29. P. Blonski, J. Hafner, *J. Phys. Condens. Matter* **23**, 136001 (2011)